Dyes and Pigments 94 (2012) 443–451

Contents lists available at SciVerse ScienceDirect

Dyes and Pigments

journal homepage: www.elsevier.com/locate/dyepig

The influence of a polyamide matrix on the halochromic behaviour of the pH-sensitive azo dye Nitrazine Yellow

Lien Van der Schueren [a], Karen Hemelsoet [b], Veronique Van Speybroeck [b], Karen De Clerck [a,*]

[a] Ghent University, Department of Textiles, Technologiepark 907, 9052 Zwijnaarde, Ghent, Belgium
[b] Ghent University, Center for Molecular Modeling, Technologiepark 903, 9052 Zwijnaarde, Ghent, Belgium

ARTICLE INFO

Article history:
Received 12 December 2011
Received in revised form
14 February 2012
Accepted 16 February 2012
Available online 28 February 2012

Keywords:
Halochromism
Azo dye
Tautomerism
Polyamide
Fiber
pH-sensor

ABSTRACT

It is of great interest to introduce pH-sensitive dyes into fibrous materials since this may result in flexible sensor systems. However, to date, the effect of a textile matrix on the halochromic properties of dyes is still unknown which severely limits their further development. Therefore, this paper focuses on an in-depth study of the halochromism of the azo pH-indicator dye Nitrazine Yellow in solution and incorporated in polyamide textile matrices with different structures. Based on both experimental spectroscopic data and computational calculations, an azo hydrazone tautomerism was found to be responsible for the halochromism of Nitrazine Yellow in solution. The hydrazone tautomer was most stable in neutral pH while the deprotonated dye molecule was believed to be an azo tautomer, resulting in a bathochromic shift with increasing pH. This tautomerism was, moreover, also present in the polyamide matrices. However, the equilibrium was clearly affected by the polymeric environment resulting in a shift and broadening of the dynamic pH-range. The polyamide type and textile structure influenced the halochromic response due to different interactions and accessibility of the dye. In conclusion, the halochromism of Nitrazine Yellow is present in all studied systems and is always based on an azo hydrazone tautomerism but the polyamide matrix causes distinct alterations in the tautomeric equilibrium.

1. Introduction

Chromism has become a booming research field in various scientific domains [1]. Also in the field of textiles, chromic materials offer major potential [2–6]. Besides the well known thermochromism and photochromism, the less exploited halochromism (or pH-sensitivity) may be of great value for various textile applications such as wound dressings, protective clothing etc [7–11]. These textile pH-sensors show advantages over the so far commonly used sensor materials thanks to their flexibility, comfort and potentially high area that can be covered. Thus far, research has, however, focused on the correlation between the chemical structure of newly developed dyes and their halochromic behaviour in solution rather than on their behaviour in a textile material [12–14]. Yet, to fully exploit the pH-sensitive function in textiles, the characterisation of the dyes as incorporated in a textile matrix is absolutely necessary. It is indeed generally recognised that a changing microenvironment affects the halochromic behaviour of dyes [15–19]. Previous preliminary studies proved the polymer type [7] as well as the porosity of the textile structure [8] to affect the halochromic response. Despite these strong indications towards the high impact of the textile matrix, no detailed literature is so far available concerning the influence of a textile material on the halochromism of pH-sensitive dyes.

In general azo dyes are the most important dye class hence also several pH-indicators are azo dyes [20]. Nitrazine Yellow, 2-(2,4-dinitrophenylazo)-1-hydroxynaphthalene-3,6-disulfonic acid disodium salt, (NY) (C.I. 5423-07-4) (Fig. 1) is an example of such an azo pH-indicator and changes colour from yellow to blue in the neutral pH-range (pH 6.0–7.0). Although there is some discussion in literature whether NY exists as an ortho- or a para-hydroxyazo [18], the ortho isomer is assumed in this paper since this is the generally accepted one. NY is a mono-azo dye containing two sulphonate groups thus showing a high similarity to acid dyes used for the colouration of polyamides. NY combined with polyamide textiles is thus an ideal candidate to study the effect of a textile matrix on the halochromism. Within the group of azo pH-indicators, the colour change is mostly based on a tautomerism. Since it is known that azo dyes containing a proton donor which is ortho or para to the azo group (such as NY) can show azo hydrazone tautomerism [21,22], the halochromism of NY is most probably

* Corresponding author. Tel.: +32 9 264 57 40; fax: +32 9 264 58 46.
E-mail addresses: lien.vanderschueren@ugent.be (L. Van der Schueren), karen.hemelsoet@ugent.be (K. Hemelsoet), veronique.vanspeybroeck@ugent.be (V. Van Speybroeck), karen.declerck@ugent.be (K. De Clerck).

0143-7208/$ – see front matter © 2012 Elsevier Ltd. All rights reserved.
doi:10.1016/j.dyepig.2012.02.013

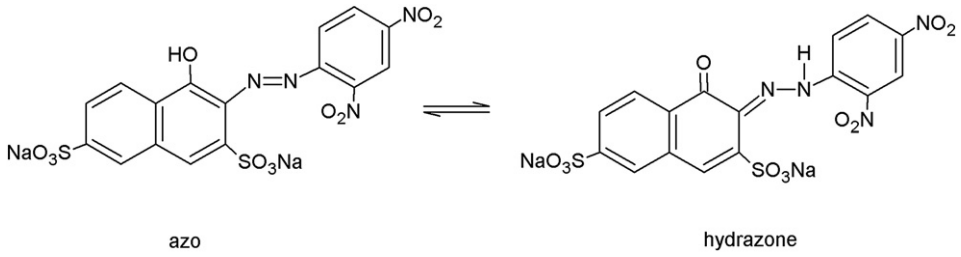

Fig. 1. Nitrazine Yellow (NY) as azo and hydrazone tautomer.

based on this principle. With this it should be kept in mind that possible interactions of the dye with the surrounding polymeric fibres may alter the tautomerism.

To study this tautomerism, a combination of experiment and theory is used in this paper [21,23]. Both gas phase simulations and continuum solvent models employing Density Functional Theory (DFT) have been applied to investigate the relative tautomer stability [24,25]. Other studies focus on the computation of the electronic spectra, aiming at an accurate reproduction of experimental electronic excitation energies thus serving as approximations for the UV–vis spectra [26–29]. In this paper, these computational techniques are combined leading to an innovative approach which deepens the understanding of the pH-sensitivity of NY.

In order to obtain a better insight into the effect of textile matrices on the halochromism of dyes, this paper focuses on an in-depth study of the selected pH-indicator dye NY applied on polyamide (PA) fabrics using an acid dyeing process. To study the influence of the fibre type, it is chosen to include both PA 6 and PA 6.6. Moreover, this paper also aims to elucidate the possible effect of the textile structure. For this purpose, not only conventional PA woven fabrics are dyed with NY but the dye is also incorporated in PA nanofibrous nonwovens. The halochromism is characterised through UV–vis spectroscopy, and Raman spectroscopic measurements are applied to investigate the molecular changes of NY upon a pH-variation. In addition, a set of computational calculations on NY are performed to obtain more insight into the energetics of the various forms of NY and to unravel the origin of the observed peaks in the UV–vis spectra. The obtained results add to the general knowledge on halochromic dyes in various environments, a key issue vital for the use of pH-sensitive dyes in textile sensors.

2. Materials and methods

2.1. Materials

Conventional PA 6 and PA 6.6 fabrics (fibre diameter 13 μm) were obtained from Concordia Textiles (Waregem, Belgium). PA 6 and PA 6.6 pellets and the solvents 98% formic acid and 99.8% acetic acid needed for producing the nanofibrous nonwovens by electrospinning were supplied by Sigma Aldrich. NY, hydrochloric acid and sodium hydroxide were also supplied by Sigma Aldrich. The complexing agent poly(diallyldimethylammonium chloride) (Perfixan RDV) was kindly supplied by Chemotex (Kortrijk, Belgium).

2.2. Methods

2.2.1. Experimental details

All dyeings were performed in a Mathis Labomat BFA-8 lab dyeing machine using an acid dyeing process (60 min at 100 °C at pH 5, set with acetic acid). Different dye concentrations were examined in the study (0.1, 0.5, 1.1 and 1.5% omf NY). After dyeing, all fabrics were dried in a conditioned room. The exhaustion was evaluated by a spectral absorption measurement of the dyeing solution before and after the dyeing process.

The water fastness of the conventional fabrics was determined according to the standard ISO 105-E01:1994 and evaluation was done using a greyscale going from 5 (best performing) to 1 (worst performing). The after treatment with the complexing agent, resulting in the formation of a complex between the anionic dye and the cationic agent, was performed at 35 °C for 30 min with 5% omf Perfixan and a liquor ratio of 20:1.

The nanofibrous nonwovens were prepared via electrospinning, which is the best established technique to produce nanofibres and which is described in detail elsewhere [30]. PA 6 polymer solutions of 16 wt% and PA 6.6 polymer solutions of 14 wt% were prepared in a 1:1 formic acid–acetic acid solvent system [31,32]. All solutions were magnetically stirred at room temperature in a closed system for 3 h. After dissolving the polyamide, a certain amount of NY (0.07, 0.46, 1.1 and 1.5% omf NY) was added to the polymer solution and the whole was again stirred for 30 min. In the electrospinning process, the flow rate was set at 2 ml h^{-1} (PA 6) and 3.5 ml h^{-1} (PA 6.6), the tip to collector distance at 6 cm and the voltage at 25 kV (using a Glassman High Voltage Series EH source). The resulting PA 6 nanofibres had on average a diameter of 244 ± 42 nm and the PA 6.6 one of 208 ± 33 nm.

To study the water fastness of the nanofibrous structures, the ISO standard is not suitable because of the small dimensions of the produced structures. Therefore, an alternative test method was applied calculating the percentage dye release. The electrospun samples were first rinsed with demineralised water. Next, 0.012 g of the samples was placed in 10 ml of demineralised water at pH 12. After 24 h the absorbance of the water solution with possible released dye was measured by UV–vis spectroscopy and finally the dye release was converted into percentage release with respect to the original amount of dye present in the structure.

pH measurements were executed with a combined reference and glass electrode (SympHony Meters VMR). Potassium nitrate with a concentration of 10^{-2} mol l^{-1} was added to ensure a constant activity coefficient during measurements. Hydrochloric acid and sodium hydroxide were used to adjust the pH.

The UV–vis spectra were recorded with a Perkin–Elmer Lambda 900 spectrophotometer. For the absorption spectra of solutions 1 cm matched quartz cells were used, for the reflection measurements on fabrics an integrated sphere (Spectralon Labsphere 150 mm) was used. The spectra were recorded from 380 nm to 780 nm with a data interval of 1 nm (absorption) and 4 nm (reflection).

The Lab values were calculated out of the UV–vis spectra by CIE-Lab using a D65/10° illuminant. The magnitude of the colour difference was quantified by ΔE (formula (1)) with ΔL the lightness difference, Δa and Δb the differences in a and b values, wherein a is a measure of redness/greenness and b of yellowness/blueness [33]. A ΔE value higher than 1 indicates a visually detectable colour difference with higher values for greater colour changes.

$$\Delta E = \sqrt{\Delta L^2 + \Delta a^2 + \Delta b^2} \quad (1)$$

Table 1
Computed difference in electronic (ΔE_{el}) and Gibbs free (ΔG^{298}) energy between the azo and hydrazone tautomers of neutral NY relative to the hydrazone form, using B3LYP/6-31+G(d,p) and C-PCM-B3LYP/6-31+G(d,p) optimized geometries for gas phase and solvent simulations, respectively. Values are in kJ/mol.

	Gas phase		Continuum water solvent
	ΔE_{el}	ΔG^{298}	ΔG^{298}
B3LYP	15.6	13.9	11.6
CAM-B3LYP	17.6	15.9	16.6

Raman spectra were recorded on a Perkin–Elmer Spectrum GX. A diode-pumped YAG near infrared laser (1064 nm), an InGaAs detector and a Raman beamsplitter were used. The measurements were performed in backscattering mode (180° excitation optics) with 64 scans (PA structures and powder) or 128 scans (aqueous solutions), a resolution of 4 cm^{-1} and a laser power of 500 mW (PA structures and aqueous solutions) or 50 mW (powder) in the spectral range 100–3500 cm^{-1} with a data interval of 1 cm^{-1}.

2.2.2. Computational details

All ab initio calculations were carried out using the Gaussian 09 software package. DFT was chosen due to its excellent cost-to-reliability performance compared to post-Hartree–Fock methods. Both the neutral hydrazone and azo tautomers of NY (Fig. 1) were investigated as models for the azo dye in acidic and neutral solutions, whereas a deprotonated compound was taken to represent the dye in alkaline environment. Continuum solvent effects were modelled using the CPCM model within self-consisted reaction field (SCRF) theory, by means of both optimizations and single-point calculations. Geometries were optimized using the hybrid B3LYP functional and 6-31+G(d,p) basis set. The long-range corrected hybrid functional CAM-B3LYP was used to perform energy refinements and time-dependent DFT (TD-DFT) computations using the ground state geometries. This theoretical methodology was previously shown to perform well for the study of similar azo dyes [28,29].

3. Results and discussion

3.1. Halochromism of NY in aqueous solution

Before elaborating on the mechanism behind the halochromism of NY in a polyamide matrix, it is essential to study the dye molecule itself and the possible presence of a tautomerism. This will serve as a starting point to the interpretation of the behaviour of the dye in combination with polymeric fibres.

DFT computations of NY provide more insight into the structural conformations responsible for the observed electronic spectrum and into the nature of the electronic transitions. The azo and hydrazone tautomer forms of neutral NY (Fig. 1) were optimized to represent the dye in an acidic and neutral environment. The obtained differences in electronic energy and Gibbs free energy at 298 K, using both the normal (B3LYP) as well as long-range corrected (CAM-B3LYP) hybrid functional for the energetics, are given in Table 1. Based on these grounds, a clear preference is found for the hydrazone form, regardless of the functional used for the computation of the energetics. Moreover, inclusion of the aqueous solvent does not alter the relative stability of the tautomers, as was also reported by Ozen et al. for similar azo compounds involving a naphthyl unit [26]. We also investigated the influence of using protons instead of sodium counter ions to balance the SO_3^- groups, however this did not alter the stability trend, the computed ΔG^{298} values differ at most by 2 kJ/mol (results are not tabulated).

A representation of the CPCM-B3LYP/6-31+G(d,p) optimized hydrazone structure is depicted in Fig. 2a, whereas Fig. 2b represents the deprotonated form of NY which can serve as a model for the dye in alkaline environment. Albeit the presence of the different substituents, the intramolecular hydrogen bonding leads to a nearly planar structure for neutral NY, whereas for the deprotonated compound a deviation from planarity is obtained. The central dihedral angle C–N–N–C equals 178° and 165° for neutral and deprotonated NY, respectively, computed at the CPCM-B3LYP/6-31+G(d,p) level of theory. Investigation of the atomic charges using the Natural Population Analysis (NPA) [34] reveals that the deprotonated compound agrees with an azo structure, since the negative charge is more located on the oxygen atom compared to the salient nitrogen atoms (see Fig. 2b). These results thus strongly suggest an azo hydrazone tautomerism at the basis of the halochromic behaviour of NY with the hydrazone form found in acidic and neutral solutions and the azo form at alkaline pH.

The colour of NY in aqueous solutions of varying pH (from pH 2–12) was recorded by UV–vis spectroscopy. Their experimental absorbance spectra are presented in Fig. 3a. The absorbance maximum varies with pH from 466 nm at acidic pH to 590 nm at alkaline pH. This corresponds to a visual colour transition from yellow to blue. Fig. 3b depicts the absorbance at 466 nm and 590 nm as a function of pH and clearly shows that the halochromic response happens in a relatively small area from pH 6 to pH 8 with a pKa value of 6.6 ± 0.1.

Electronic transitions of the neutral, hydrazone tautomer and deprotonated NY are studied using TD-DFT computations on the ground state geometry. The first electronic transitions are found at 449 and 640 nm, respectively (Fig. 4). The calculated value of the neutral compound is thus in satisfactory agreement with the experimentally obtained value of 466 nm. Moreover, a clear bathochromic shift, in agreement with the experimental shift, is found

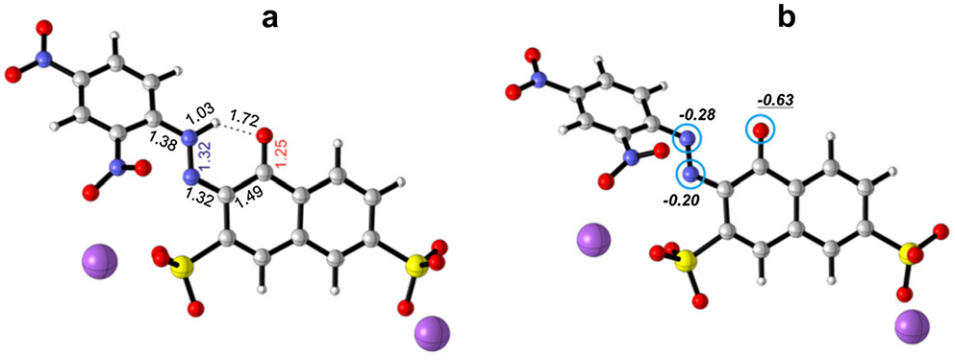

Fig. 2. (a) Optimized CPCM-B3LYP/6-31+G(d,p) geometry of the hydrazone form of neutral NY. Bond lengths are given in Å. (b) Optimized CPCM-B3LYP/6-31+G(d,p) geometry of deprotonated NY with indication of NPA atomic charges.

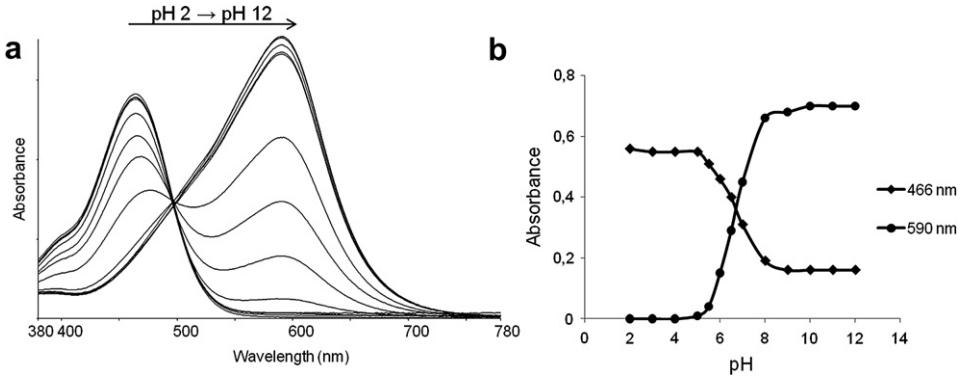

Fig. 3. (a) Absorbance spectra at varying pH and (b) Absorbance as a function of pH at 466 nm and 590 nm of NY in an aqueous solution.

in the case of deprotonation, representative of the alkaline environment. The computed first excitation energies predominantly result from a HOMO to LUMO transition ($\pi \rightarrow \pi^*$ transition) (Fig. 4).

Also the experimental Raman spectra (Fig. 5a) confirm the proposed azo hydrazone tautomerism. The peak at 1615 cm^{-1} can be attributed to a combination of ring vibrations and C=O stretching [35,36], the latter being only possible in the hydrazone form of the molecule (Fig. 1). This peak is present at pH 2, 4 and 6 and disappears at pH 8 while the peak at 1598 cm^{-1}, most likely attributed to phenyl and naphthyl ring vibrations of the azo form, appears at pH 8 and higher [22,35–37]. Further, the peak at 1514 cm^{-1}, which can be related to C=N stretching of the hydrazone form is present from pH 2 to 6 and is not seen at higher pH [22,36]. Finally, a peak at 1384 cm^{-1}, which corresponds to N=N stretching and thus to the azo form of NY [35,38–40], arises at pH 8. In addition the Raman spectra show the narrow pH-range in which the halochromism occurs since only between pH 6 and pH 8 changes in the Raman peaks are observed.

3.2. Specification of NY in polyamide matrices

A thorough discussion on the spectral behaviour of NY in the dry state together with an analysis of the water fastness of the dyed textiles is essential to allow and to clearly interpret the halochromic study which will be discussed in Section 3.3. Therefore, PA 6 and PA 6.6 conventional woven fabrics were dyed with NY at dye concentrations from 0.1 to 1.5% omf by a standard acid dyeing process. The exhaustion values followed the expected trends of decreasing exhaustion with increasing dye concentration and of higher exhaustions for PA 6 compared to PA 6.6. The latter is caused by the higher number of amino end groups on PA 6 giving more possible dyeing sites and thus higher exhaustions [41]. Moreover, PA 6 shows a more amorphous and thus more open structure also leading to higher exhaustion values [42]. Of surprise was the substantial change in hue with increasing dye concentration for both PA's as shown in Fig. 6. At low dye concentrations the peak at 618 nm dominated thus giving a bluish green colour while at higher concentrations the peak at 474 nm was the dominant one giving a green colour. The variation in *b* value calculated according to CIE Lab (D65/10) confirmed this trend with an increase in *b* value and thus a less bluish colour with increasing concentration (*b* value of −9.1 for 0.1% omf NY to 16.5 for 1.5% omf NY).

These clear variations in hue with varying dye concentration are probably related to accessibility differences between the different dyed fabrics. During dyeing, the NY molecules are in the acidic and thus yellow form because of the acid dyeing process. At low dye

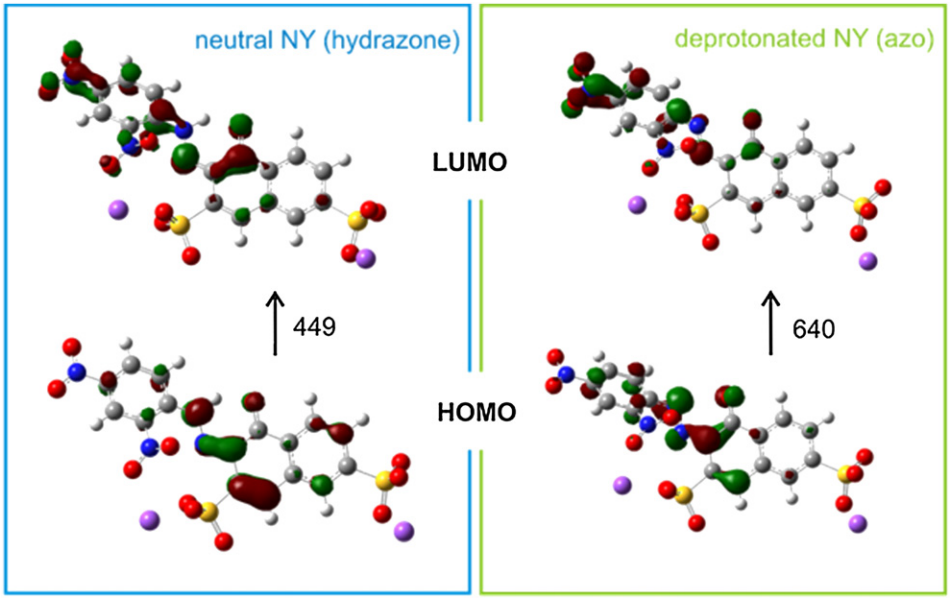

Fig. 4. First electronic transitions (in nm) of the neutral hydrazone and deprotonated azo form of NY, computed using CPCM-CAM-B3LYP/6-31+G(d,p) TD-DFT computations on CPCM-B3LYP/6-31+G(d,p) optimized geometries. Isosurfaces of the involved HOMO and LUMO orbitals are also depicted.

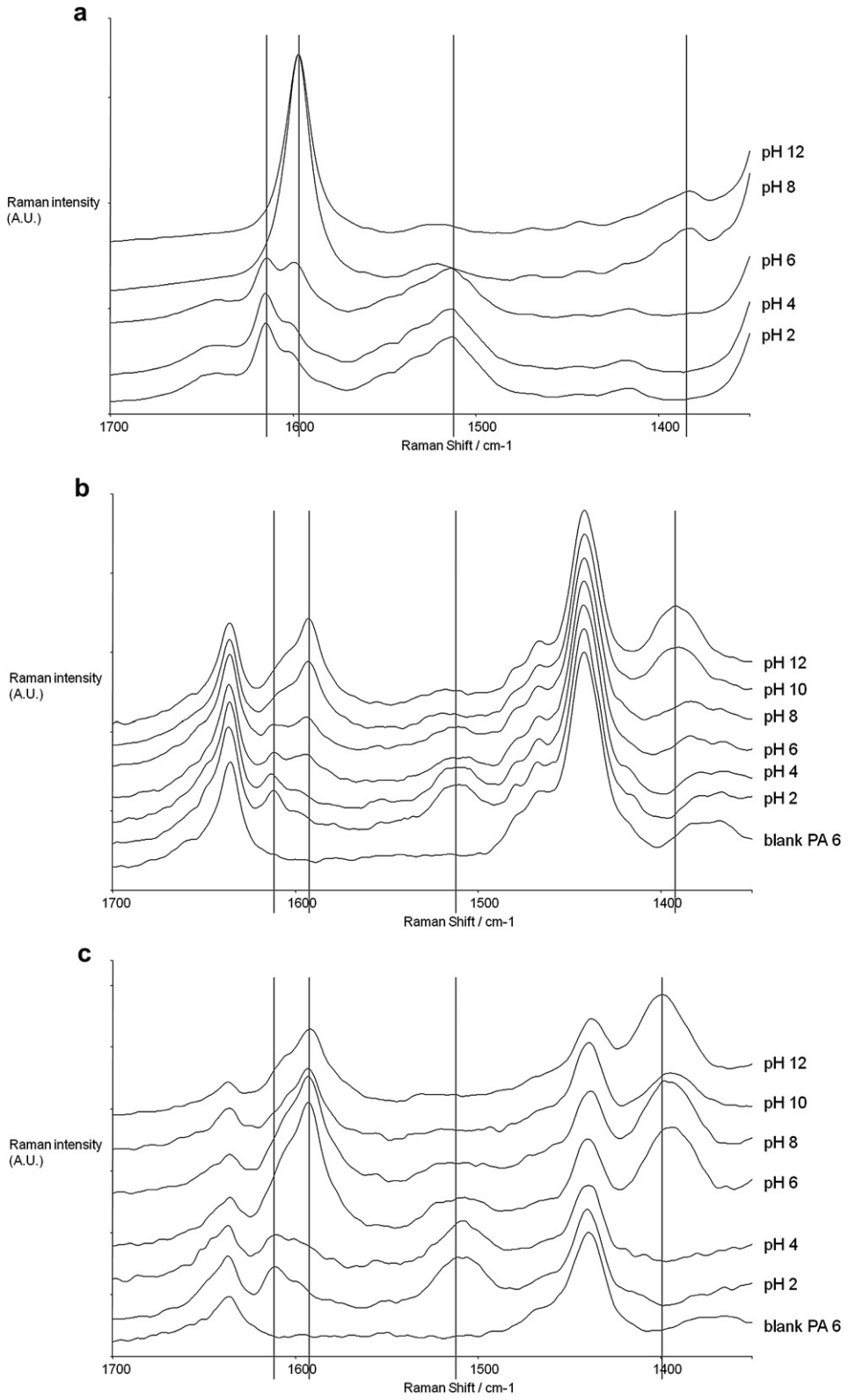

Fig. 5. Raman spectra as a function of pH of (a) NY in aqueous solutions, (b) NY in PA 6 fabrics (1.5% omf), normalised at 1440 cm^{-1}, (c) NY in PA 6 nanofibrous nonwovens (1.5% omf), normalised at 1440 cm^{-1}.

concentrations the dye molecules in the PA fabric are most likely easily accessible leading to a change to a bluish green colour, in agreement with the colour of the dye in an aqueous solution at neutral pH. On the other hand, at higher NY concentrations, part of the dye molecules are probably difficult to access leading to a green colour as a mixture of the acidic (yellow) and alkaline (blue) molecular structure of NY. Since PA 6 shows a more open and thus more accessible structure than PA 6.6, a higher relative peak intensity of the 618 nm peak to the 474 nm peak is found until higher dye concentrations (Fig. 6). Further, also dye aggregation,

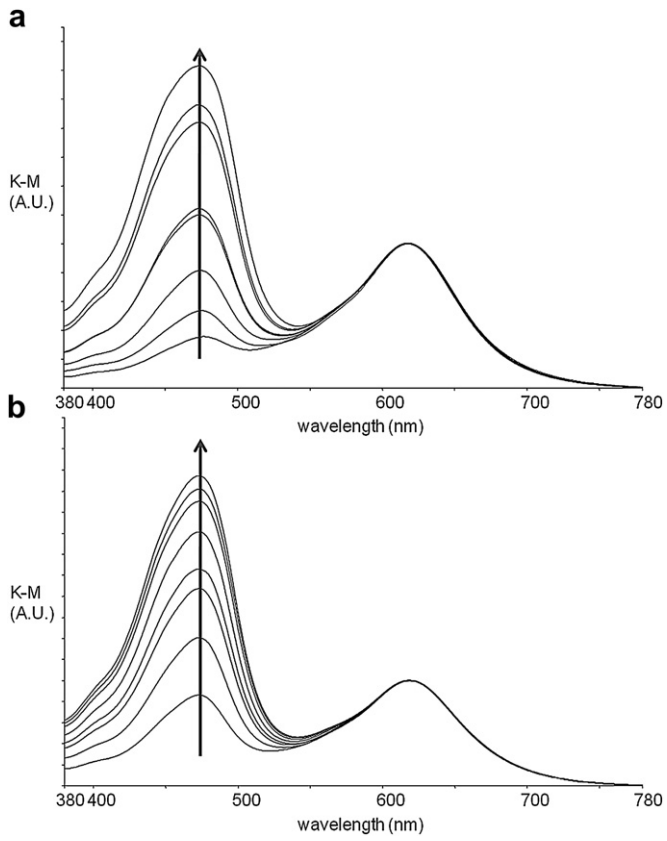

Fig. 6. Kubelka-Munk spectra of PA 6 (a) and PA 6.6 (b) fabric dyed with NY, normalised at 618 nm. Arrow indicates increasing dye concentration.

which is known to be more prevalent at higher dye concentrations, may be partly responsible. The hydrazone form of NY shows a higher planarity (Section 3.1) and the dye molecules are thus more liable to dye aggregation at an acidic pH. These aggregates might not be able to readily turn into the alkaline form leading to the appearance of a green colour [43,44]. Finally, also the type of dye–fibre interactions vary upon dye concentration causing different hues. The NY molecules are probably mainly bound by ionic interactions at lower dye concentrations. However, at higher concentrations, part of the dye molecules interact with PA by dipole–dipole and hydrophobic interactions.

Next, the water fastness of the obtained fabrics was determined. The results, presented in Table 2, show that the fastness significantly decreased with increasing dye concentration. Only with a very low concentration (0.1% omf) could good water fastness values be obtained. The dye molecules are strongly bound at lower dye concentrations thanks to the ionic interactions. However, at higher concentrations, also weaker interactions are present resulting in a higher dye release. By applying an after treatment with the complexing agent, the water fastness for all NY concentrations was notably improved (Table 2).

As to be able to study the behaviour of NY in different textile structures, it was aimed to also dye nanofibrous structures produced by electrospinning. The exhaustions of this dyeing process were very high for all concentrations (close to 100%) due to the high specific surface area of nanofibrous structures. This high specific surface area, however, also caused extremely poor water fastnesses with an almost complete removal of all dye molecules. Previous studies showed that nanofibrous structures can be efficiently coloured with pH-sensitive dyes by electrospinning a polymer solution to which the dyes are added before the start of the process [8]. This colouration approach was thus also successfully applied in our study. No substantial change in hue – only in colour depth – with concentration was found indicating that all NY molecules, regardless of the dye concentration, can easily be reached and assume an equal structure. This is related to the small diameter of the nanofibres and their high specific surface area.

The percentage dye release of the nanofibrous samples was measured for two different NY concentrations (0.5 and 1.5% omf) and both for PA 6 and PA 6.6 in a water bath at pH 12. Dye release was observed at all pH values but was substantially higher at alkaline pH due to the decrease in planarity (Section 3.1) and in ionic interactions [8]. Hence this high pH-value allows for an accurate measurement of the dye release. The nanofibrous structures showed a particularly high release up to 87% as observed in Table 3. To improve this, 4% omf complexing agent was added to the PA electrospinning solutions. The dye release indeed decreased substantially (Table 3) and samples loaded with the complexing agent thus allow for the halochromic study in Section 3.3.

3.3. Halochromism of NY in PA matrices

3.3.1. Halochromism of NY in conventional dyed PA fabrics

The investigation of the halochromic behaviour of NY incorporated in PA fabrics was performed by immersion of the samples in aqueous pH baths. To minimize the dye release during these experiments, it was recommended to work with the fabrics treated with the complexing agent. The discussion thus focuses on the latter samples.

The PA 6 fabrics showed a reversible colour transition with pH from yellow to blue. The maximum time lag for this response was 20 min with shorter time lags at extreme pH values (e.g. pH 2). All Kubelka–Munk spectra of PA 6 with different NY concentrations showed an acidic maximum at 477 nm and an alkaline at 615 nm. Also the pH-range in which the transition occurs is not influenced by the NY concentration. This is clearly demonstrated by the variation in ΔE value with respect to pH 2 (calculated using formula (1)) which shows a distinct variation between pH 3 and 10 for both 0.1

Table 2
Assessment of the water fastness using a greyscale of PA 6 and PA 6.6 dyed with NY, before and after a treatment with a complexing agent (5: best performing, 1: worst performance).

% omf NY	PA 6		PA 6, after treated		PA 6.6		PA 6.6, after treated	
	Adjacent PA	Adjacent wool	Adjacent PA	Adjacent wool	Adjacent PA	Adjacent wool	Adjacent PA	Adjacent wool
0.1	5	5	5	5	5	5	5	5
0.3	3/4	5	4/5	5	3/4	5	4	5
0.5	2	4	3/4	5	2	4	3	4/5
0.7	2	3	3	4/5	2	3	2/3	4/5
0.9	1/2	2	3	4/5	2	2	2/3	4/5
1.1	1/2	2	3	4/5	2	2	2/3	4/5
1.3	1/2	2	2/3	4/5	1/2	2	2	4/5
1.5	1/2	2	2/3	4/5	1/2	2	2	4/5

Table 3
The dye release (in % with respect to the original amount of dye) at pH 12 for PA 6 and PA 6.6 nanofibrous structures, with and without loading with complexing agent.

PA type	% omf NY	% Dye release	
		Without agent	With agent
PA 6	0.46	75.1	2.6
	1.5	87.3	39.7
PA 6.6	0.54	75.0	8.8
	1.5	69.8	19.8

and 1.5% omf NY (Fig. 7a). However, the relative peak intensities of the acidic and alkaline maxima do change with NY concentration with a higher relative intensity for the 615 nm peak relative to the 477 nm peak for lower dye concentrations thus resulting in a more bluish colour at high pH. The corresponding *b* values of the Lab colour space are thus lower for lower NY concentrations as confirmed in Fig. 7b. This agrees well with the results found on the PA 6 fabrics measured after dyeing in Section 3.2 and is again believed to be attributed to accessibility difficulties of dye molecules entrapped within the fibres and possible dye aggregation.

The halochromism of PA 6.6 fabrics did not demonstrate major differences compared to PA 6. The maximum wavelengths were again found at 477 and 615 nm and also the pH-range in which the colour change occurred did not alter as seen in Fig. 7c. However, in agreement with the colour measurements of the fabrics after dyeing (Section 3.1), a less bluish colour was observed for PA 6.6 than for PA 6 with thus corresponding higher *b* values (Fig. 7d). This results in a lower maximum ΔE value for the colour difference between pH 2 and pH 12 (48.1 for PA 6 compared to 42.4 for PA 6.6 and this for 1.5% omf NY dyed fabrics).

The halochromic behaviour of NY clearly changed after incorporation in a textile matrix compared with the solution. While the halochromic response in aqueous solutions happened within 2 pH units (pH 6–8), the response in PA 6 and PA 6.6 fabrics occurred in a much broader range from pH 3 to 10. Also the acidic and alkaline wavelength maxima altered after incorporation in a PA matrix. Both maxima show a bathochromic shift of 11 nm and 25 nm respectively. These changes are attributed to a varying microenvironment as already stated for other systems which use a pH-sensitive dye in a certain environment such as e.g. a silica matrix [15,45]. The azo hydrazone tautomerism in specific is known to be influenced not only by structural factors within the molecule, but also by the nature of the medium surrounding the molecules [46].

Raman measurements, performed on 1.5% omf NY PA 6 fabric (Fig. 5b) showed the same overall trends as NY in aqueous solution, meaning a decreasing 1613 cm^{-1} peak, an increasing 1594 cm^{-1} peak, a decreasing 1511 cm^{-1} peak and an increasing 1392 cm^{-1} peak with increasing pH. This thus suggests that the azo hydrazone tautomerism remains responsible for the halochromism of NY in PA 6. However, while in solution a sharp transition between the Raman spectra at pH 6 and 8 is present, a broader pH-range in which changes in Raman peaks occur is seen in PA 6. This agrees well with the data from the visible spectra and indicates a broader pH area consisting of a mixture of the hydrazone and azo structure of NY. Moreover, also small shifts in the position of the Raman peaks of NY are observed after incorporation in PA, hence indicating interactions between NY and the polymeric fibres. Raman spectra of dyed PA 6.6 fabrics were generally similar to those of PA 6.

3.3.2. *Halochromism of NY in nanofibrous nonwovens*

Analogous to the conventional dyed PA fabrics, only the halochromism of nanofibrous nonwovens loaded with NY in the presence of the complexing agent are discussed. Nanofibrous NY structures showed a small response time with a response within 5 min. This is significantly shorter compared to the NY conventional fabrics which is attributed to the high specific surface area, high porosity and small diameter of nanofibrous nonwovens leading to an easy accessibility of the dyes and thus a fast response.

All PA 6 nonwovens with NY visually and reversibly changed colour from yellow to blue with increasing pH. However, contrary to the conventional PA 6 fabrics, the dye concentration does influence the halochromic response of PA 6 nanofibres. This is clearly depicted in Fig. 8a showing a sharp transition in ΔE value

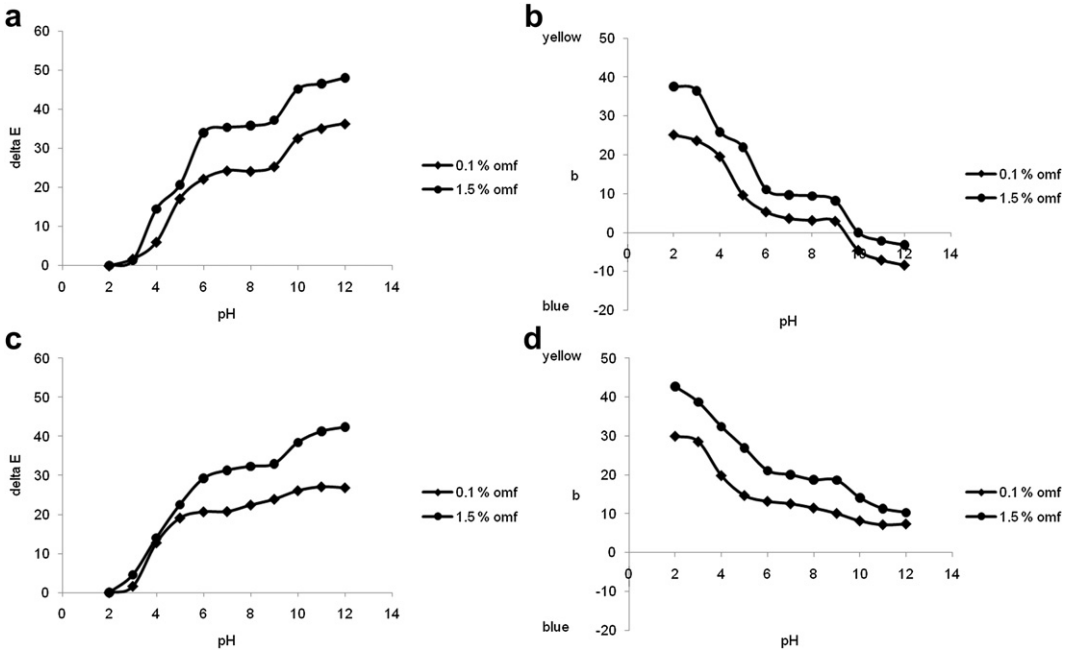

Fig. 7. (a) ΔE value with respect to pH 2 as a function of pH of PA 6 fabric dyed with NY, (b) *b* value as a function of pH of PA 6 fabric dyed with NY, (c) ΔE value with respect to pH 2 as a function of pH of PA 6.6 fabric dyed with NY, (d) *b* value as a function of pH of PA 6.6 fabric dyed with NY.

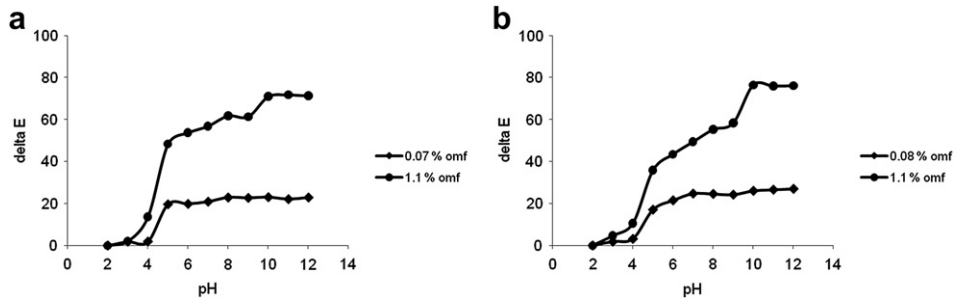

Fig. 8. (a) ΔE value with respect to pH 2 as a function of pH of PA 6 nanofibrous nonwoven with NY and (b) of PA 6.6 nanofibrous nonwoven with NY.

between pH 4 and 6 for 0.07% omf NY and a broad transition between pH 3 and 10 for 1.1% omf. The halochromic behaviour of nanofibres at 1.1% omf is thus similar to the behaviour of conventional fabrics as observed in Figs. 7 and 8a. In contrast, the transition at 0.07% omf is similarly sharp as the transition in solution with yet an acidic shift of two pH units (pH 4 to 6 compared to pH 6 to 8 in solution).

Also the visible spectra demonstrate a higher similarity to the solution at lower dye concentrations. The alkaline maximum shifts with the dye concentration from 615 nm at 1.1% omf to 603 nm at 0.07% omf. Hence the bathochromic shift with respect to the solution decreases from 25 nm (1.1% omf) to 13 nm (0.07% omf). The resemblance to the behaviour in solution at low dye concentration is probably related to the easy accessibility of the small amount of NY molecules present in the fibres, leading to a fast response of all molecules. In contrast, a part of the NY molecules in a conventional woven PA fabric and in nanofibres at high dye concentrations might be difficult to access leading to a different response for different dye molecules and thus a broader pH-range. Moreover, at low dye concentrations, a greater proportion of the NY molecules is believed to be well dispersed while aggregation might occur at higher concentrations possibly resulting in unreacting dye molecules.

Again, the peak variations of the Raman spectra (of 1.5% omf NY PA 6), Fig. 5c, suggest an azo hydrazone tautomerism at the basis of the halochromism of NY. However the peak at 1594 cm^{-1} is already present at pH 6 while the peak at 1613 cm^{-1} already completely disappeared at this pH-value. Also the Raman band at 1396 cm^{-1} is clearly visible at pH 6 which was not the case for NY in solution and in conventional PA 6 fabrics. These data thus indicate that the azo form of NY is formed at lower pH-values in nanofibrous nonwovens compared to the solution.

In general almost no differences were observed between the behaviour of PA 6 and PA 6.6 nanofibrous nonwovens as seen in Fig. 8. In contrast to the conventional fabrics, no differences in *b* values and thus in bluish appearance of the samples were noticed indicating that the high porosity of the nonwovens overcomes the less open structure of PA 6.6 compared to PA 6. Also in the Raman spectra no differences between PA 6 and PA 6.6 were observed. The above results prove that not only the polymer type may have an influence on the halochromic properties but also the fibrous structure of the polymeric material plays an important role.

4. Conclusion

In this paper, the halochromic behaviour of the pH-indicator NY was investigated. Ab initio calculations of the neutral and deprotonated dye molecule proved a preference for the hydrazone form in acidic and neutral circumstances, whereas a deprotonated compound exhibiting typical characteristics of the azo form was a good model in alkaline circumstances. Raman spectroscopic spectra of NY solutions at different pH-values confirmed these calculations. Moreover, Raman spectra of the dyed polyamide samples proved that the azo hydrazone tautomerism is also present in the polyamide matrices. Yet, shifts of the positions of the Raman peaks and changes in the variations of specific peaks with pH with regard to the solution, do suggest interactions between PA and NY affecting its halochromism.

Also the experimental visible spectra showed that the surrounding polymeric environment has an obvious effect on the halochromism of NY. A broadening of the dynamic pH-range was observed together with a shift in the wavelength maxima of NY. Moreover, the halochromic behaviour of conventional PA 6 and PA 6.6 fabrics was affected by the dye concentration. The pH-range of the response did not alter but a less bluish colour was observed at higher dye concentrations. A less blue colour was also found for PA 6.6 compared to PA 6. These changes in bluish appearance were believed to be due to accessibility differences between both the different dye concentrations and the different PA types. Also dye aggregation can partly explain these experimental observations. No differences between PA 6 and PA 6.6 were noticed on nanofibrous nonwovens thanks to their high porosity and thus easy accessibility. Lower dye concentrations however still exhibited a different behaviour on nanofibrous samples than higher dye concentrations. Yet, all polyamide samples showed a clear colour shift upon a pH-variation and are hence regarded as promising colorimetric textile sensors.

This paper proves the high relevance of studying the impact of polymeric matrices on the halochromic properties of dyes. The methodology used can also be applied for other dyes and polymer types which will thus further enlarge the fundamental knowledge on interactions between dyes and fibres and aid to the practical development of pH-sensitive fibrous sensors.

Acknowledgements

The Research Board of Ghent University (BOF) and the Fund for Scientific Research – Flanders (FWO) are acknowledged for their financial support.

References

[1] Bamfield P. Chromic phenomena, technological applications of colour chemistry. 1st ed. Cambridge: RSC: Royal Society of Chemistry; 2001.
[2] Marcin R. Thermochromic cellulose fibers. Polym Adv Technol 2007;18:323–8.
[3] Oda H. Photostabilization of organic thermochromic pigments. Part 2: effect of hydroxyarylbenzotriazoles containing an amphoteric counter-ion moiety on the light fastness of color formers. Dyes Pigm 2008;76:400–5.
[4] Son YA, Park YM, Park SY, Shin CJ, Kim SH. Exhaustion studies of spiroxazine dye having reactive anchor on polyamide fibers and its photochromic properties. Dyes Pigm 2007;73:76–80.
[5] Christie RM, Hepworth JD, Gabbutt CD, Rae S. An investigation of the electronic spectral properties of the coloured photoproducts derived from some photochromic naphtho[2,1-b]pyrans. Dyes Pigm 1997;35:339–46.
[6] Little AF, Christie RM. Textile applications of photochromic dyes. Part 1: establishment of a methodology for evaluation of photochromic textiles using

traditional colour measurement instrumentation. Color Technol 2010;126:157–63.
[7] Van der Schueren L, De Clerck K. The use of pH-indicator dyes for pH-sensitive textile materials. Text Res J 2010;80:590–603.
[8] Van der Schueren L, Mollet T, Ceylan Ö, De Clerck K. The development of polyamide 6.6 nanofibres with a pH-sensitive function by electrospinning. Eur Polym J 2010;46:2229–39.
[9] Trupp S, Alberti M, Carofiglio T, Lubian E, Lehmann H, Heuermann R, et al. Development of pH-sensitive indicator dyes for the preparation of micropatterned optical sensor layers. Sens Actuators B Chem 2010;150:206–10.
[10] Staneva D, Betcheva R. Synthesis and functional properties of new optical pH sensor based on benzo[de]anthracen-7-one immobilized on the viscose. Dyes Pigm 2007;74:148–53.
[11] Staneva D, Betcheva R, Chovelon JM. Optical sensor for aliphatic amines based on the simultaneous colorimetric and fluorescence responses of smart textile. J Appl Polym Sci 2009;106:1950–6.
[12] Thirumurugan P, Muralidharan D, Perumal PT. The synthesis and photophysical studies of quinoxaline and pyridopyrazine derivatives. Dyes Pigm 2009;81:245–53.
[13] Jaung JY. Synthesis and halochromism of new quinoxaline fluorescent dyes. Dyes Pigm 2006;71:245–50.
[14] Griffiths J, Cox R. Colour and halochromic properties of azo dyes derived from 10-methyl-9-methylene-9,10-dihydroacridine as coupling component. Dyes Pigm 2000;47:65–71.
[15] Ertekin K, Karapire C, Alp S, Yenigul B, Icli S. Photophysical and photochemical characteristics of an azlactone dye in sol-gel matrix; a new fluorescent pH-indicator. Dyes Pigm 2003;56:125–33.
[16] Liu Z, Luo F, Chen T. Phenolphthalein immobilized membrane for an optical pH sensor. Anal Chim Acta 2004;510:189–94.
[17] Morris D, Coyle S, Wu YZ, Lau KT, Wallace G, Diamond D. Bio-sensing textile based patch with integrated optical detection system for sweat monitoring. Sens Actuators B Chem 2009;139:231–6.
[18] Viscardi G, Quagliotto P, Barolo C, Caputo G, Digilio G, Degani L, et al. Structural characterisation of Nitrazine Yellow by NMR spectroscopy. Dyes Pigm 2003;57:87–95.
[19] Van der Schueren L, De Clerck K. Textile materials with a pH-sensitive function. Int J Cloth Sci Tech 2011;23:269–74.
[20] Waring DR, Hallas G. The chemistry and application of dyes. 1st ed. New York: Plenum Press; 1990.
[21] Pavlovic G, Racane L, Cicak H, Tralic-Kulenovic V. The synthesis and structural study of two benzothiazolyl azo dyes: X-ray crystallographic and computational study of azo-hydrazone tautomerism. Dyes Pigm 2009;83:354–62.
[22] Abbott LC, Batchelor SN, Oakes J, Gilbert BC, Whitwood AC, Smith JRL, et al. Experimental and computational studies of structure and bonding in parent and reduced forms of the azo dye orange II. J Phys Chem A 2005;109:2894–905.
[23] Mataza D, Ando R, Borin A, Santos P. Azo-hydrazone tautomerism in protonated aminoazobenzenes: resonance Raman spectroscopy and quantum-chemical calculations. J Phys Chem A 2008;112:4437–42.
[24] Abbott LC, Batchelor SN, Oakes J, Smith JRL, Moore JN. Semiempirical and ab initio studies of the structure and spectroscopy of the azo dye direct blue 1: comparison with experiment. J Phys Chem A 2004;108:10208–18.
[25] Teimouri A, Chermahini AN, Taban K, Dabbagh HA. Exerpimental and CIS, TD-DFT, ab initio calculations of visible spectra and the vibrational frequencies of sulfonyl azide-azoic dyes. Spectrochim Acta A 2009;72:369–77.
[26] Ozen AS, Doruker P, Aviyente V. Effect of cooperative hydrogen bonding in azo-hydrazone tautomerism of azo dyes. J Phys Chem A 2007;111:13506–14.
[27] Guillaumont D, Nakamura S. Calculation of the absorption wavelength of dyes using time-dependent density-functional theory (TD-DFT). Dyes Pigm 2000;46:85–92.
[28] Jacquemin D, Perpete EA, Scuseria GE, Ciofini I, Adamo C. TD-DFT performance for the visible absorption spectra of organic dyes: conventional versus long-range hybrids. J Chem Theory Comput 2008;4:123–35.
[29] Jacquemin D, Preat J, Perpete EA, Vercauteren DP, Andre JM, Ciofini I, et al. Absorption spectra of azobenzenes simulated with time-dependent density functional theory. Int J Quantum Chem 2011;111:4224–40.
[30] Greiner A, Wendorff J. Electrospinning: a fascinating method for the preparation of ultrathin fibers. Angew Chem Int Ed 2007;46:5670–703.
[31] De Vrieze S, Westbroek P, Van Camp T, De Clerck K. Solvent system for steady state electrospinning of polyamide 6.6. J Appl Polym Sci 2009;115:837–84.
[32] De Schoenmaker B, Van der Schueren L, De Vrieze S, Westbroek P, De Clerck K. Wicking properties of various polyamide nanofibrous structures with an optimized method. J Appl Polym Sci 2011;120:305–10.
[33] Zollinger H. Color chemistry. 2nd ed. Cambridge: VCH; 1991.
[34] Reed AE, Curtiss LA, Weinhold F. Intermolecular interactions from a natural bond orbital, donor–acceptor viewpoint. Chem Rev 1988;88:899–926.
[35] Dines TJ, MacGregor LD, Rochester CH. A resonance Raman spectroscopic study of the protonation of 2-(4′-hydroxyazo)-benzoic acid adsorbed on oxide surfaces. Vib Spectros 2003;32:225–40.
[36] Snehalatha M, Ravikumar C, Hubert Joe I. Spectroscopic investigation and ab initio computations of the dye chromotrope 2R. Solid State Sci 2009;11:1275–82.
[37] Snehalatha M, Ravikumar C, Hubert Joe I, Sekar N, Jayakumar VS. Spectroscopic analysis and DFT calculations of a food additive carmoisine. Spectrochim Acta A 2009;72:654–62.
[38] Jia TJ, Song G, Li PW, He TC, Mo YJ, Cui YT. Vibrational modes study of methyl orange using SERS-measurement and the DFT method. Mod Phys Lett B 2008;22:2869–79.
[39] Biswas N, Umapathy S. Structures, vibrational frequencies, and normal modes of substituted azo dyes: infrared, Raman and density functional calculations. J Phys Chem A 2000;104:2734–45.
[40] Cataliotti RS, Morresi A, Paliani G. Resonance Raman scattering in azo dyes. J Raman Spectros 1989;20:601–4.
[41] Satake M, Mido Y. Chemistry of colour. 1st ed. New Delhi: Discovery Publishing House; 2003.
[42] Aspland JR. Textile dyeing and coloration. 1st ed. North Carolina: American Association of Textile Chemists and Colorists; 1997.
[43] Bredereck K, Schumacher C. Structure reactivity correlations of azo reactive dyes based on H-acid: I NMR chemical-shift values, pKa values, dyestuff aggregation and dyeing behaviour. Dyes Pigm 1993;21:23–43.
[44] Epolito WJ, Lee YH, Bottomley LA, Pavlostathis SG. Characterization of the textile anthraquinone dye reactive blue 4. Dyes Pigm 2005;67:35–46.
[45] Jurmanovic S, Kordic S, Steinberg MD, Murkovic Steinberg I. Organically modified silicate thin films doped with colourimetric pH-indicators methyl red and bromocresol green as pH-responsive sol–gel hybrid materials. Thin Solid Films 2010;518:2234–40.
[46] Ball P, Nicholls CH. Azo-hydrazone tautomerism of hydroxyazo compounds – a review. Dyes Pigm 1982;3:5–26.